

Research Article

# Evaluation of apparent diffusion coefficient measurements and magnetic resonance imaging findings in benign and malignant gynecologic masses

## *Benign ve malign jinekolojik kitlelerde görünen difüzyon katsayısı ölçümlerinin ve manyetik rezonans görüntüleme bulgularının değerlendirilmesi*

İD Büşra Şeker\*<sup>1</sup>, İD Gökhan Yılmaz<sup>2</sup>, İD Nisa Başpınar<sup>1</sup>, İD Begüm Kurt<sup>3</sup>, İD Orhan Solak<sup>1</sup>

<sup>1</sup>Department of Radiology, Cumhuriyet University, Faculty of Medicine, Sivas, Turkey

<sup>2</sup>Department of Radiology, İstinye University Hospital, İstanbul, Turkey

<sup>3</sup>Department of Obstetrics and Gynaecology, Cumhuriyet University, Faculty of Medicine, Sivas, Turkey

### Abstract

**Aim:** This study aimed to investigate the differences in magnetic resonance imaging (MRI) findings and various apparent diffusion coefficient (ADC) measurements between benign and malignant gynecologic masses.

**Material and Methods:** MRI images of 102 patients with pelvic masses, examined between June 2016 and November 2018, were retrospectively reviewed. Patients were categorized histopathologically as benign or malignant, by lesion composition (cystic, solid, mixed), and according to anatomical location (ovary, uterus, tube, cervix). Three ADC measurement methods were applied: diffuse ADC (dADC) from large ROIs covering the entire lesion, focal ADC (fADC) from small ROIs placed on the darkest regions of each slice, and specific ADC (sADC) calculated as the mean of the three lowest fADC values.

**Results:** According to lesion composition, solid lesions demonstrated lower ADC values than mixed lesions, yet no differences were observed between benign and malignant categories within each lesion composition. In ovarian and uterine masses, the value of ADCs showed no significant differences between benign and malignant groups. For cervical masses, the mean ADCs were higher in benign masses compared to malignant masses (dADC:  $2.4 \pm 0.2$  vs.  $1.1 \pm 0.3$ ,  $p=0.002$ ; fADC:  $2.3 \pm 0.2$  vs.  $0.7 \pm 0.1$ ,  $p=0.001$ ; sADC:  $2.2 \pm 0.2$  vs.  $0.6 \pm 0.02$ ,  $p=0.001$ ).

**Conclusion:** Among various ADC measurement strategies, focal and specific ADC values more clearly reflected diffusion differences between benign and malignant gynecologic masses, particularly in cervical lesions. ADC values were affected by lesion composition, yet within each composition subgroup, benign and malignant lesions exhibited comparable values.

**Keywords:** Gynecologic masses, diffusion-weighted imaging, apparent diffusion coefficient, malignant, cervical cancer

Corresponding Author\*: Büşra Şeker, Department of Radiology, Cumhuriyet University, Faculty of Medicine, Sivas, Turkey

E-mail: busrasoylu.obs@gmail.com

Orcid: 0000-0001-7766-4276

Doi: 10.18663/tjcl.1724174

Received: 23.06.2025 accepted: 30.06.2025

## Öz

**Amaç:** Bu çalışma, benign ve malign jinekolojik kitleler arasında manyetik rezonans görüntüleme (MRG) bulguları ve çeşitli görünen difüzyon katsayısı (ADC) ölçümleri açısından farkları araştırmayı amaçlamaktadır.

**Gereç ve Yöntemler:** Haziran 2016 ile Kasım 2018 tarihleri arasında incelenen, pelvik kitleye sahip 102 hastanın MRG görüntüleri retrospektif olarak değerlendirildi. Hastalar histopatolojik olarak benign (n=82) veya malign (n=20) şeklinde, lezyon kompozisyonuna (kistik, solid, mikst) ve anatomik lokalizasyona (over, uterus, tüp, serviks) göre sınıflandırıldı. Üç ADC ölçüm yöntemi uygulandı: tüm lezyonu kapsayan geniş ROI'lerden elde edilen diffüz ADC (dADC), her kesitteki en koyu bölgelere yerleştirilen küçük ROI'lerden elde edilen fokal ADC (fADC) ve en düşük üç fADC değerinin ortalaması olarak hesaplanan spesifik ADC (sADC).

**Bulgular:** Lezyon kompozisyonuna göre solid lezyonlar, mikst lezyonlardan daha düşük ADC değerleri gösterdi, ancak her bir lezyon kompozisyonunda benign ve malign kategoriler arasında farklılık gözlenmedi. Over ve uterin kitlelerde, ADC değerleri benign ve malign gruplar arasında anlamlı fark göstermedi. Servikal kitlelerde benign lezyonların ortalama ADC değerleri malign gruba kıyasla daha yüksekti (dADC için  $2,4 \pm 0,2$  ve  $1,1 \pm 0,3$ ,  $p=0,002$ ; fADC için  $2,3 \pm 0,2$  ve  $0,7 \pm 0,1$ ,  $p=0,001$ ; sADC için  $2,2 \pm 0,2$  ve  $0,6 \pm 0,02$ ,  $p=0,001$ ).

**Sonuç:** Farklı ADC ölçüm yöntemleri arasında, özellikle servikal lezyonlarda, fokal ve spesifik ADC değerleri benign ve malign jinekolojik kitleler arasındaki difüzyon farklılıklarını daha açık şekilde yansıtmıştır. ADC değerleri lezyon kompozisyonundan etkilense de her kompozisyon alt grubunda iyi huylu ve kötü huylu lezyonlar benzer değerler gösterdi.

**Anahtar kelimeler:** Jinekolojik kitleler, difüzyon ağırlıklı görüntüleme, görünen difüzyon katsayısı, malign, servikal kanser

## Introduction

Gynecological masses originating in the ovaries, uterus, fallopian tubes, or cervix present a common diagnostic challenge, as accurate preoperative differentiation between benign and malignant lesions is crucial for guiding appropriate management. The main goal of imaging evaluation is to distinguish malignant tumors from benign ones and thereby determine the optimal surgical or therapeutic strategy [1, 2]. Magnetic resonance imaging (MRI) provides excellent soft-tissue contrast and detailed anatomical information for characterizing pelvic masses; however, even with high-resolution conventional MRI, reliably predicting malignancy can be difficult [3-5]. This limitation has prompted growing interest in advanced MRI techniques such as diffusion-weighted imaging (DWI) to improve lesion characterization.

DWI is an MRI sequence that quantifies the random motion of water molecules within tissues, and the derived apparent diffusion coefficient (ADC) values offer a quantitative measure of tissue cellularity and integrity. Malignant tumors often contain densely packed, hypercellular tissue that restricts water diffusion, causing markedly lower ADC values relative to less cellular benign lesions [6-8]. By incorporating ADC measurements into routine pelvic MRI protocols, radiologists can move beyond purely morphological assessment and potentially improve the distinction between benign and

malignant gynecologic masses. In addition to its diagnostic value, ADC is also used to determine treatment response and prognosis during chemotherapy [9-11].

We hypothesize that malignant gynecological masses exhibit distinct quantitative ADC values and conventional MRI characteristics compared to benign lesions, and that ADC measurements can improve diagnostic accuracy in differentiating these entities. Therefore, the aim of this study is to investigate whether conventional MRI findings and quantitative ADC values differ between benign and malignant gynecological masses.

## Material And Methods

This retrospective study was conducted using data from patients who underwent magnetic resonance imaging (MRI) with a preliminary diagnosis of pelvic mass at the Department of Radiology, Cumhuriyet University Faculty of Medicine, between June 2016 and November 2018. The study was approved by the Cumhuriyet University Non-Interventional Clinical Research Ethics Committee (Date: 20.02.2019, Approval No: 2019-02/26) and was carried out in accordance with the relevant ethical guidelines and the Helsinki Declaration (2013 Brazil revision). The need for informed consent was waived under the approval of the Local Ethics Committee due to the retrospective design.

During the study period, 115 patients who underwent MRI

examinations due to a preliminary diagnosis of pelvic mass were retrospectively evaluated. Inclusion criteria encompassed individuals aged from 15 to 94 years who had pelvic masses identified, accompanied by postoperative histopathology results and clinical follow-up data. After applying exclusion criteria, specifically the absence of pelvic mass detection ( $n = 7$ ) or missing histopathological and clinical follow-up records ( $n = 6$ ), a total of 102 patients were enrolled in the final analysis.

### Study Protocol

The hospital's electronic information system and patient files were used to gather demographic and clinical data. Imaging findings of the patients were collected via the Picture Archiving and Communication System (PACS).

Pelvic MRI and diffusion MRI examinations were conducted using a 1.5 Tesla MRI system (Magnetom Aera, Siemens, Erlangen, Germany) equipped with a dedicated body coil. The standard pelvic MRI protocol included T1A-weighted imaging (TR=484 ms, TE=12 ms, slice thickness 5 mm), T2A-weighted imaging (TR=3880 ms, TE=96 ms, slice thickness 5 mm), fat-suppressed T2 sequences (TR=4210 ms, TE=95 ms, slice thickness 5 mm), HASTE imaging from T2 sequences (TR=1400 ms, TE=102 ms, slice thickness 6 mm), and VIBE imaging from fat-suppressed T1 sequences (TR=6.69 ms, TE=2.39 ms, slice thickness 3 mm). DWI was performed with TR=5700 ms, TE=104 ms, and slice thickness 5 mm.

### MRI Evaluation of Pelvic Masses

Pelvic masses detected via MRI were categorized based on anatomical origin into four groups: uterine, ovarian, tubal, and cervical. Additionally, lesions were classified according to their nature as solid, cystic, or mixed. Lesion sizes were measured in three dimensions (transverse, anterior-posterior, and craniocaudal), and their volumes were calculated. T1- and T2-weighted signal characteristics of lesions, along with the presence of hemorrhagic foci, were also assessed. After intravenous contrast administration, lesions were evaluated for staining characteristics and classified into four enhancement patterns: homogeneous, heterogeneous, circumferential, and septal enhancement.

### Diffusion-weighted Imaging and ADC Measurement

DWI was routinely performed before contrast administration using single-shot echo-planar imaging with diffusion-sensitive gradients applied at three b-values (50, 400, and 800  $\text{mm}^2/\text{s}$ ) along the x, y, and z axes. ADC maps were generated automatically. Three different ADC measurement approaches

were used. First, a circular region of interest (ROI)  $\geq 37 \text{ mm}^2$  was placed in each axial slice covering the lesion, and the average ADC value (diffuse ADC; dADC) was calculated. Second, focal ADC (fADC) was measured by placing a smaller ROI of 10  $\text{mm}^2$  specifically on the darkest region within each axial slice. Lastly, the specific ADC (sADC) was calculated as the arithmetic mean of the three lowest focal ADC values (Figure 1-4).

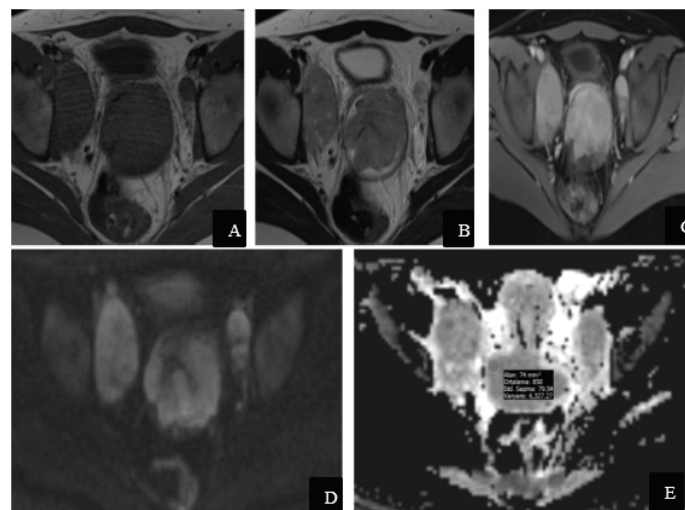


**Figure 1.** Solid lesion located in the uterine cervix. The lesion is hypointense on T1-weighted (A) and T2-weighted (B) images, measuring 50×43×27 mm (transverse × anterior-posterior × craniocaudal). It demonstrates intense homogeneous enhancement on post-contrast T1-weighted images (C). Areas of diffusion restriction are observed at  $b=1000 \text{ s/mm}^2$  on DWI (D), with a mean ADC value of  $0.66 \times 10^{-3} \text{ mm}^2/\text{s}$  measured on the ADC map (E). Histopathological diagnosis: Squamous cell carcinoma.

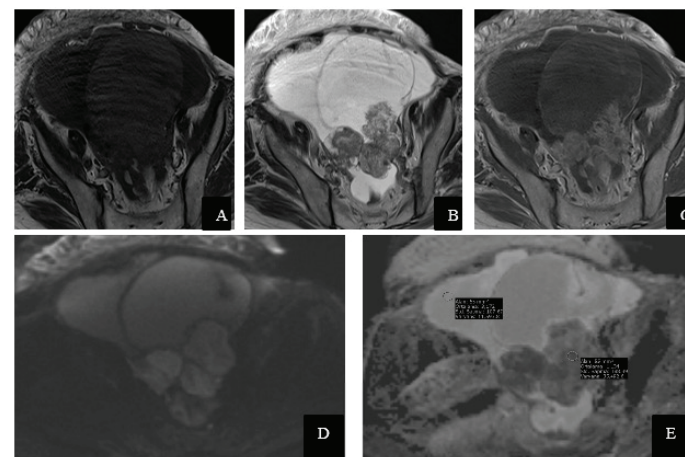


**Figure 2.** Mixed solid-cystic lesion located in the pelvic region. The lesion has lobulated contours and measures 156×102×122 mm (anterior-posterior × medial-lateral × craniocaudal), demonstrating hypointensity on T1-weighted images (A) and heterogeneous hyperintensity on T2-weighted images (B). Solid components and

septa show intense enhancement on post-contrast T1-weighted imaging (C). Prominent diffusion restriction is observed in the solid components at  $b=1000 \text{ s/mm}^2$  on DWI (D), with an average ADC value of  $1.13 \times 10^{-3} \text{ mm}^2/\text{s}$  measured on the ADC map (E). Histopathological diagnosis: Tubal serous carcinoma.

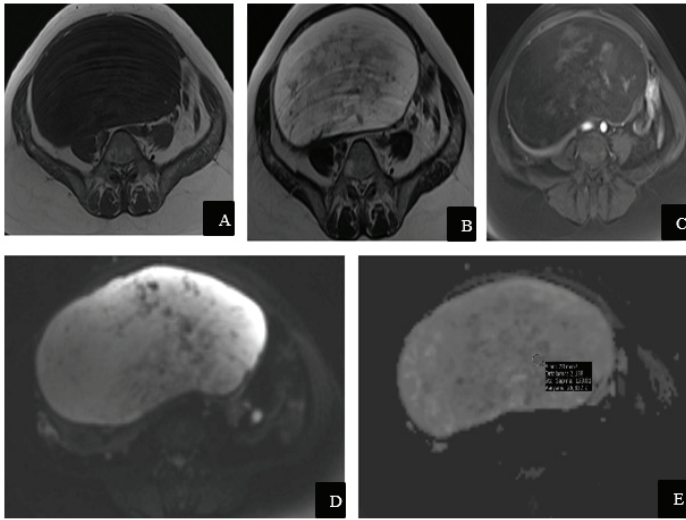


**Figure 3.** A pelvic mass originating from the uterine parenchyma, filling the pelvic cavity. The lesion measures  $242 \times 125 \times 271 \text{ mm}$  (craniocaudal  $\times$  anterior-posterior  $\times$  transverse) and is characterized as expansile and solid with well-defined borders. It is hypointense on T1-weighted (A) and heterogeneously hyperintense with cystic necrotic areas on T2-weighted images (B). On post-contrast T1-weighted imaging (C), heterogeneous enhancement is observed predominantly in the central regions. DWI at  $b=1000 \text{ s/mm}^2$  (D) shows diffusion restriction, with an ADC value of  $2.18 \times 10^{-3} \text{ mm}^2/\text{s}$  measured on the ADC map (E). Histopathological diagnosis: Cystic degenerated leiomyoma.

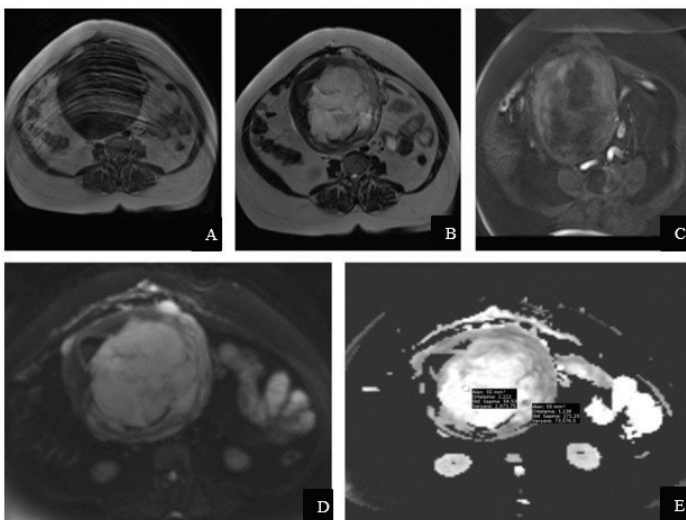


**Figure 4.** Solid uterine lesion characterized as a well-circumscribed, expansile mass measuring  $93 \times 53 \times 52 \text{ mm}$  (transverse  $\times$  anterior-posterior  $\times$  craniocaudal). It demonstrates hypointensity on T1-weighted (A) and heterogeneous hyperintensity on T2-weighted

images (B). Post-contrast T1-weighted imaging (C) reveals cystic necrotic areas and intense enhancement within the solid portions of the lesion. Areas of diffusion restriction are seen at  $b=1000 \text{ s/mm}^2$  on DWI (D), with an ADC value of  $1.13 \times 10^{-3} \text{ mm}^2/\text{s}$  measured on the ADC map (E). Histopathological diagnosis: Leiomyosarcoma.

MRI and DWI findings, including ADC values, were compared between histologically confirmed benign and malignant pelvic masses. Additionally, separate comparative analyses were performed to assess the diagnostic accuracy of MRI, DWI, and ADC metrics specifically for ovarian and uterine lesions.

### Statistical Analysis

The SPSS 26.0 (IBM Corporation, Armonk, New York, United States) program was used to analyze the variables. The conformity of the data to the normal distribution was evaluated with the Shapiro-Wilk test. Quantitative variables were summarized as mean  $\pm$  standard deviation (SD) and categorical variables as frequency and percentage. Continuous variables were compared between benign and malignant groups using the Independent-Samples T-test for normally distributed data and the Mann-Whitney U test for non-normally distributed data. A p-value below 0.05 was considered statistically significant.

### Results

A total of 102 masses were evaluated, including 82 benign and 20 malignant cases. Out of 102 cases, 91 underwent surgery, while 11 were followed clinically. Among the 55 ovarian lesions assessed, benign lesions accounted for 48 cases, including 14 endometriomas, 10 simple ovarian cysts, 7 mature cystic teratomas, 5 hemorrhagic cysts, 5 fibrothecomas, 3 mucinous cystadenomas, 3 serous papillary cystadenofibromas, and 1 serous cystadenoma. The 7 malignant lesions included 4 serous carcinomas, 2 Krukenberg tumors, and 1 Sertoli-Leydig cell tumor. Thirty-three uterine lesions comprised 28 leiomyomas, 3 endometrial cancers, and 2 leiomyosarcomas. Of the 11 cervical masses identified, 6 benign lesions were Nabothian cysts, and the remaining 5 were malignant squamous cell cervical cancers.

The mean age of patients with malignant masses was higher than those with benign masses ( $54.3 \pm 19.1$  vs.  $40.3 \pm 13.6$  years,  $p=0.001$ ). Malignant masses were predominantly mixed (60.0%), while benign masses were mostly cystic (57.3%). The ovary was the most common localization overall (53.9%), although malignancies occurred notably more frequently in cervical (25.0%). Regarding pitting patterns, malignant masses most commonly showed heterogeneous patterns (85.0%),

while no pitting pattern was detected in 47.6% of benign lesion. There was no significant difference between benign and malignant masses in terms of mean dADC values (both  $1.7 \pm 0.7$ ,  $p = 0.903$ ). However, mean fADC ( $1.1 \pm 0.6$  vs.  $1.5 \pm 0.7$ ,  $p = 0.025$ ) and mean sADC values ( $0.9 \pm 0.5$  vs.  $1.4 \pm 0.7$ ,  $p = 0.026$ ) were significantly lower in malignant masses compared to benign ones. The demographic and clinical characteristics of patients are given in Table 1.

In solid and mixed masses, the mean ADC values showed no significant differences between benign and malignant

groups (Table 2). In ovarian and uterine masses, the value of ADCs showed no significant differences between benign and malignant groups. For cervical masses, the mean ADCs were higher in benign masses compared to malignant masses ( $2.4 \pm 0.2$  vs.  $1.1 \pm 0.3$ ,  $p = 0.002$  for dADC;  $2.3 \pm 0.2$  vs.  $0.7 \pm 0.1$ ,  $p = 0.001$  for fADC;  $2.2 \pm 0.2$  vs.  $0.6 \pm 0.02$ ,  $p = 0.001$  for sADC) (Table 3). Additionally, the normal cervical stroma of 10 control cases without cervical involvement was evaluated, and the mean ADC values were as follows: diffuse ADC,  $1.7 \pm 0.3 \times 10^{-3} \text{ mm}^2/\text{s}$ ; focal ADC,  $1.7 \pm 0.2 \times 10^{-3} \text{ mm}^2/\text{s}$ ; specific ADC,  $1.7 \pm 0.7 \times 10^{-3} \text{ mm}^2/\text{s}$ .

**Table 1.** Demographic characteristics and ADC values of benign versus malignant masses.

Variables	All population n = 102	Benign n = 82	Malign n = 20	P-value
Age, years	43.0 $\pm$ 15.6	40.3 $\pm$ 13.6	54.3 $\pm$ 19.1	0.001*
Nature, n (%)				
Cystic	47 (46.1)	47 (57.3)	-	0.001*
Solid	33 (32.3)	25 (30.5)	8 (40.0)	
Mixed	22 (21.6)	10 (22.2)	12 (60.0)	
Localization				
Ovary	55 (53.9)	48 (58.5)	7 (35.0)	<0.001*
Uterus	33 (32.3)	28 (34.2)	5 (25.0)	
Tuba	3 (2.9)	-	3 (15.0)	
Cervix	11 (10.8)	6 (7.3)	5 (25.0)	
Pitting pattern				
No	39 (38.3)	39 (47.6)	-	0.001*
Homogeneous	5 (4.9)	4 (4.9)	1 (5.0)	
Heterogeneous	45 (44.1)	28 (34.1)	17 (85.0)	
Environmental	10 (9.8)	8 (9.8)	2 (10.0)	
Septal	3 (2.9)	3 (3.7)	-	
Diffuse ADC, $\times 10^{-3} \text{ mm}^2/\text{sn}$	1.7 $\pm$ 0.7	1.7 $\pm$ 0.7	1.7 $\pm$ 0.7	0.903
Focal ADC, $\times 10^{-3} \text{ mm}^2/\text{sn}$	1.4 $\pm$ 0.7	1.5 $\pm$ 0.7	1.1 $\pm$ 0.6	0.025*
Specific ADC, $\times 10^{-3} \text{ mm}^2/\text{sn}$	1.3 $\pm$ 0.7	1.4 $\pm$ 0.7	0.9 $\pm$ 0.5	0.026*

**Table 2.** Comparison of ADC values in solid and mixed masses by malignancy status.

Nature	Benign	Malign	P-value
Solid	n = 25	n = 8	
Diffuse ADC, $\times 10^{-3} \text{ mm}^2/\text{sn}$	1.1 $\pm$ 0.3	1.0 $\pm$ 0.2	0.846
Focal ADC, $\times 10^{-3} \text{ mm}^2/\text{sn}$	0.8 $\pm$ 0.3	0.8 $\pm$ 0.2	0.609
Specific ADC, $\times 10^{-3} \text{ mm}^2/\text{sn}$	0.8 $\pm$ 0.2	0.8 $\pm$ 0.3	0.918
Mixed	n = 10	n = 12	
Diffuse ADC, $\times 10^{-3} \text{ mm}^2/\text{sn}$	1.7 $\pm$ 0.6	2.0 $\pm$ 0.8	0.125
Focal ADC, $\times 10^{-3} \text{ mm}^2/\text{sn}$	1.2 $\pm$ 0.5	1.3 $\pm$ 0.6	0.667
Specific ADC, $\times 10^{-3} \text{ mm}^2/\text{sn}$	1.0 $\pm$ 0.5	1.1 $\pm$ 0.6	0.578

**Table 3.** Comparison of ADC values in the differentiation of benign and malignant according to localization.

Localization	Benign	Malign	P-value
Ovary	n = 48	n = 7	
Diffuse ADC, $\times 10^{-3}$ mm <sup>2</sup> /sn	$1.8 \pm 0.7$	$2.2 \pm 0.6$	0.172
Focal ADC, $\times 10^{-3}$ mm <sup>2</sup> /sn	$1.6 \pm 0.7$	$1.7 \pm 0.7$	0.951
Specific ADC, $\times 10^{-3}$ mm <sup>2</sup> /sn	$1.5 \pm 0.8$	$1.4 \pm 0.7$	0.814
Uterus	n = 28	n = 5	
Diffuse ADC, $\times 10^{-3}$ mm <sup>2</sup> /sn	$1.4 \pm 0.5$	$1.5 \pm 0.5$	0.679
Focal ADC, $\times 10^{-3}$ mm <sup>2</sup> /sn	$1.0 \pm 0.3$	$0.9 \pm 0.2$	0.268
Specific ADC, $\times 10^{-3}$ mm <sup>2</sup> /sn	$0.9 \pm 0.3$	$0.8 \pm 0.2$	0.458
Cervix	n = 6	n = 5	
Diffuse ADC, $\times 10^{-3}$ mm <sup>2</sup> /sn	$2.6 \pm 0.6$	$1.1 \pm 0.3$	0.002*
Focal ADC, $\times 10^{-3}$ mm <sup>2</sup> /sn	$2.5 \pm 0.2$	$0.7 \pm 0.1$	0.001*
Specific ADC, $\times 10^{-3}$ mm <sup>2</sup> /sn	$2.5 \pm 0.3$	$0.6 \pm 0.2$	0.001*

## Discussion

This study provides valuable insight into the role of diffusion-weighted MRI in characterizing pelvic masses by employing three distinct ADC measurement strategies. We defined dADC as the average ADC from a large ROI encompassing the entire lesion, fADC as the ADC from small ROIs placed on the darkest (most diffusion-restricted) region of the lesion on each slice, and sADC as the mean of the three lowest fADC values. This approach captures tumor heterogeneity by comparing whole-lesion diffusion with the most restricted areas. ADC values did not differ significantly between benign and malignant groups based on the nature (solid, cystic, mixed) of the lesions. However, a significant difference was noted in ADC values according to lesion localization, specifically within cervical lesions, where malignant lesions exhibited lower ADC values compared to benign lesions.

In our cohort, patients with malignant masses were significantly older on average than those with benign lesions (mid-50s vs. early 40s), and the malignant tumors more frequently exhibited complex mixed (solid-cystic) morphology with heterogeneous internal characteristics. These clinical and imaging features are recognized red flags for malignancy and are consistent with prior observations that adnexal and cervical malignancies tend to occur at older ages and often present with solid components on imaging [12-14]. Despite these features, our diffusion MRI results highlight a nuanced picture. Despite solid masses having lower ADC values than mixed masses, these values did not significantly differ between benign and malignant groups. Also, ovarian and uterine lesions showed no ADC value differences between benign and malignant classifications. However, malignant cervical lesions exhibited significantly lower ADC values compared to their benign counterparts.

Solid masses tend to have markedly lower ADC values than lesions with cystic portions. The reason is that a completely solid tumor affords little free space for water movement – water molecules are hindered by cell membranes, intracellular organelles, and sometimes fibrous matrix. By contrast, if a tumor is mixed (solid-cystic) or contains cystic areas (fluid-filled regions), the fluid allows relatively unhindered Brownian motion of water, which drives the ADC upward in those areas. In practical terms, a simple fluid-filled cyst will appear bright on an ADC map (high ADC) since water diffusion is nearly free, whereas a densely cellular solid tumor nodule appears dark on the ADC map (low ADC) due to restricted diffusion [15, 16]. Numerous studies have confirmed this dichotomy: cystic tumor components exhibit higher ADC values than solid tumor components (this holds true for both benign and malignant lesions) [1]. Rousell et al. evaluated 54 pelvic masses, measuring ADC separately from cystic and solid components. Mean ADC values for benign and malignant lesions from cystic components were  $2. \pm 0.5 \times 10^{-3}$  mm<sup>2</sup>/s and  $2. \pm 0.5 \times 10^{-3}$  mm<sup>2</sup>/s, without significant differences. Similarly, solid component ADC values for benign and malignant lesions were  $1.2 \pm 0.6 \times 10^{-3}$  mm<sup>2</sup>/s and  $1.0 \pm 0.2 \times 10^{-3}$  mm<sup>2</sup>/s, respectively, also showing no significant difference [17]. The results of our study are consistent with these observations.

In ovarian and uterine masses, the differences in diffusion metrics between benign and malignant lesions were not statistically significant. One likely explanation is the overlap in ADC values caused by lesion heterogeneity. Certain benign ovarian tumors such as fibromas, teratomas and endometriomas) can exhibit unusually low ADC values due to their contents, overlapping with the restricted diffusion seen in malignancies [1, 18]. Granular studies have found,

for example, that the mean ADC of solid components was not significantly different between benign and malignant ovarian tumors in some series [16]. Similarly, benign uterine fibroids with dense fibrous tissue may show very low ADC (a “T2 blackout” effect), mimicking the diffusion restriction of uterine sarcomas [19]. Tamai et al. observed that sarcomas had lower average ADC values than normal myometrium and degenerated leiomyomas with no overlap. However, they noted overlapping ADC values with ordinary and cellular leiomyomas [20]. These overlapping diffusion patterns diminish the statistical separation between benign and malignant groups, which aligns with recent studies reporting conflicting or inconclusive ADC findings in ovaries and uterus when lesion composition is diverse.

In contrast, cervical lesions showed clear and significant differences in all three ADC measures between benign and malignant cases. Cervical cancers are typically highly cellular, and this dense cell packing markedly restricts water diffusion, resulting in much lower ADC values in malignant tumors compared to normal or benign cervical tissue [21]. Previous studies have identified mean ADC values of about  $1.0\text{--}1.1 \times 10^{-3} \text{ mm}^2/\text{s}$ , which are considerably lower than those observed in normal cervical stroma, typically between  $1.5\text{--}2.1 \times 10^{-3} \text{ mm}^2/\text{s}$  [22–25]. Differences by histology have also been observed – squamous cell carcinomas typically show slightly lower ADC values than adenocarcinomas, a finding attributed to histologic differences (e.g. squamous tumors often being more densely cellular, whereas adenocarcinomas may have glandular mucin that increases water diffusivity) [26]. The current study did not allow comparisons across different histological types because of insufficient sample numbers. Although the dADC values for cervical lesions obtained in our study were consistent with the literature, our findings indicate that the fADC and sADC measurements demonstrated more substantial differences. In effect, the true tissue diffusion coefficient (slow ADC/dADC) drops in cancers, and even the perfusion-related diffusion component is reduced: intravoxel incoherent motion analysis confirms that both the pure diffusivity  $D$  and the perfusion fraction  $f$  are significantly lower in cervical carcinomas compared to normal cervical tissue [27]. These microstructural differences make ADC a valuable diagnostic biomarker in cervical cancer. Importantly, ADC values also carry prognostic information. Lower ADC tends to correlate with more aggressive tumor features – for instance, well-differentiated (Grade I) cervical cancers showed significantly higher ADC ( $\sim 1.04 \times 10^{-3} \text{ mm}^2/\text{s}$ ) than poorly differentiated Grade III tumors (approx.  $0.67 \times 10^{-3} \text{ mm}^2/\text{s}$ )

[28]. Similarly, the most diffusion-restricted tumors often indicate aggressive pathology: lesions with lymphovascular space invasion have significantly lower minimum ADC than tumors without lymphovascular invasion [29]. Consistently, pretreatment ADC has been linked to outcomes: tumors with very low ADC (high diffusion restriction) are associated with greater risk of recurrence and poorer survival, whereas higher ADC values tend to portend a more favorable prognosis [30].

This study has several limitations. First, its retrospective and single-center design introduces a potential selection bias and may limit the generalizability of the findings to broader populations. Second, the sample size—especially the number of malignant lesions—was relatively small, which may limit the statistical power of subgroup analyses, particularly those stratified by localization (e.g., cervix, ovary, uterus). Third, ROI placement was performed manually, and despite efforts to standardize it, some degree of subjectivity in selecting the darkest areas or lesion borders is inevitable. Fourth, lesion composition was heterogeneous within each group; for example, benign ovarian lesions included both simple cysts and endometriomas, which may have different diffusion characteristics despite falling under the same histopathological category. Finally, histological subtypes and tumor grades—particularly among malignant cases—were not analyzed separately, though these features are known to influence ADC values and may partially explain intragroup variability. These limitations suggest that further prospective studies with larger, balanced cohorts and blinded, multi-reader designs are warranted to validate the diagnostic and prognostic performance of ADC metrics in gynecological masses.

## Conclusion

ADC values in gynecologic masses can vary based on the nature of masses and anatomical structures evaluated. Solid lesions and malignant cervical masses typically show lower ADC measurements. However, in ovarian and uterine lesions, considerable overlap in ADC values limited diagnostic performance, highlighting the need for cautious interpretation. While focal ROI strategies may enhance the sensitivity of DWI for detecting malignancy, ADC values alone are insufficient as stand-alone diagnostic tools due to lesion heterogeneity and compositional variability. Therefore, ADC metrics should be integrated with conventional MRI findings and clinical context for a more accurate and comprehensive evaluation of gynecologic masses.

## Funding

The authors declared that this study has received no financial support.

## Conflicts of Interest

The authors declare they have no conflicts of interest.

## Ethics Approval

The study was performed in accordance with the Declaration of Helsinki, and was approved by the Cumhuriyet University Non-Interventional Clinical Research Ethics Committee (Date: 20.02.2019, Approval No: 2019-02/26).

## Informed Consent

The need for informed consent was waived under the approval of the Local Ethics Committee due to the retrospective design.

## Availability of Data and Material

The data that support the findings of this study are available on request from the corresponding author.

## Authors' contribution

Concept – B.Ş. and O.S., Design- B.Ş. and O.S., Data collection and/or processing – B.Ş., G.Y., N.B., and O.S., Analysis and/or interpretation – B.Ş., G.Y., N.B., and O.S., Writing – B.Ş., Critical review- B.Ş., G.Y., N.B., and O.S. All authors read and approved the final version of the manuscript.

## Reference

1. Kim HJ, Lee SY, Shin YR, Park CS, and Kim K. The Value of Diffusion-Weighted Imaging in the Differential Diagnosis of Ovarian Lesions: A Meta-Analysis. *PLoS One*. 2016;11(2):e0149465. DOI: 10.1371/journal.pone.0149465.
2. Chandramohan A, Bhat TA, John R, and Simon B. Multimodality imaging review of complex pelvic lesions in female pelvis. *Br J Radiol*. 2020;93(1116):20200489. DOI: 10.1259/bjr.20200489.
3. Vargas HA, Barrett T, and Sala E. MRI of ovarian masses. *J Magn Reson Imaging*. 2013;37(2):265-81. DOI: 10.1002/jmri.23721.
4. Lin R, Hung YY, Cheng J, and Suh-Burgmann E. Accuracy of Magnetic Resonance Imaging for Identifying Ovarian Cancer in a Community-Based Setting. *Womens Health Rep (New Rochelle)*. 2022;3(1):43-48. DOI: 10.1089/whr.2021.0106.
5. Salman S, Shireen N, Riyaz R, Khan SA, Singh JP, and Uttam A. Magnetic resonance imaging evaluation of gynecological mass lesions: A comprehensive analysis with histopathological correlation. *Medicine (Baltimore)*. 2024;103(32):e39312. DOI: 10.1097/MD.00000000000039312.
6. Manoharan D, Das CJ, Aggarwal A, and Gupta AK. Diffusion weighted imaging in gynecological malignancies - present and future. *World J Radiol*. 2016;8(3):288-97. DOI: 10.4329/wjrv.8.3.288.
7. Dhanda S, Thakur M, Kerkar R, and Jagmohan P. Diffusion-weighted imaging of gynecologic tumors: diagnostic pearls and potential pitfalls. *Radiographics*. 2014;34(5):1393-416. DOI: 10.1148/rg.345130131.
8. Mukuda N, Fujii S, Inoue C, et al. Apparent diffusion coefficient (ADC) measurement in ovarian tumor: Effect of region-of-interest methods on ADC values and diagnostic ability. *J Magn Reson Imaging*. 2016;43(3):720-5. DOI: 10.1002/jmri.25011.
9. Gladwish A, Milosevic M, Fyles A, et al. Association of Apparent Diffusion Coefficient with Disease Recurrence in Patients with Locally Advanced Cervical Cancer Treated with Radical Chemotherapy and Radiation Therapy. *Radiology*. 2016;279(1):158-66. DOI: 10.1148/radiol.2015150400.
10. Marconi DG, Fregnani JH, Rossini RR, et al. Pre-treatment MRI minimum apparent diffusion coefficient value is a potential prognostic imaging biomarker in cervical cancer patients treated with definitive chemoradiation. *BMC Cancer*. 2016;16:556. DOI: 10.1186/s12885-016-2619-0.
11. Onal C, Guler OC, and Yildirim BA. Prognostic Use of Pretreatment Hematologic Parameters in Patients Receiving Definitive Chemoradiotherapy for Cervical Cancer. *Int J Gynecol Cancer*. 2016;26(6):1169-75. DOI: 10.1097/IGC.0000000000000741.
12. Ali MN, Habib D, Hassanien AI, and Abbas AM. Comparison of the four malignancy risk indices in the discrimination of malignant ovarian masses: A cross-sectional study. *J Gynecol Obstet Hum Reprod*. 2021;50(5):101986. DOI: 10.1016/j.jogoh.2020.101986.
13. Gala FB, Gala KB, and Gala BM. Magnetic Resonance Imaging of Uterine Cervix: A Pictorial Essay. *Indian J Radiol Imaging*. 2021;31(2):454-67. DOI: 10.1055/s-0041-1734377.
14. Oh H, Park SB, Park HJ, et al. Ultrasonographic features of uterine cervical lesions. *Br J Radiol*. 2021;94(1121):20201242. DOI: 10.1259/bjr.20201242.
15. Duarte AL, Dias JL, and Cunha TM. Pitfalls of diffusion-weighted imaging of the female pelvis. *Radiol Bras*. 2018;51(1):37-44. DOI: 10.1590/0100-3984.2016.0208.
16. Liu R, Li R, Fang J, et al. Apparent diffusion coefficient histogram analysis for differentiating solid ovarian tumors. *Front Oncol*. 2022;12:904323. DOI: 10.3389/fonc.2022.904323.
17. Roussel A, Thomassin-Naggara I, Darai E, Marsault C, and Bazot M. [Value of diffusion-weighted imaging in the evaluation of adnexal tumors]. *J Radiol*. 2009;90(5 Pt 1):589-96. DOI: 10.1016/s0221-0363(09)74025-9.
18. Fujii S, Kakite S, Nishihara K, et al. Diagnostic accuracy of diffusion-weighted imaging in differentiating benign from malignant ovarian lesions. *J Magn Reson Imaging*. 2008;28(5):1149-56. DOI: 10.1002/jmri.21575.
19. Kim H, Rha SE, Shin YR, et al. Differentiating Uterine Sarcoma From Atypical Leiomyoma on Preoperative Magnetic Resonance Imaging Using Logistic Regression Classifier: Added Value of Diffusion-Weighted Imaging-Based Quantitative Parameters. *Korean J Radiol*. 2024;25(1):43-54. DOI: 10.3348/kjr.2023.0760.



20. Tamai K, Koyama T, Saga T, et al. The utility of diffusion-weighted MR imaging for differentiating uterine sarcomas from benign leiomyomas. *Eur Radiol.* 2008;18(4):723-30. DOI: 10.1007/s00330-007-0787-7.
21. Rizescu RA, Salcianu IA, Ionescu A, et al. The Added Role of Diffusion-Weighted Magnetic Resonance Imaging in Staging Uterine Cervical Cancer. *Cureus.* 2024;16(12):e75707. DOI: 10.7759/cureus.75707.
22. Chen J, Zhang Y, Liang B, and Yang Z. The utility of diffusion-weighted MR imaging in cervical cancer. *Eur J Radiol.* 2010;74(3):e101-6. DOI: 10.1016/j.ejrad.2009.04.025.
23. Naganawa S, Sato C, Kumada H, Ishigaki T, Miura S, and Takizawa O. Apparent diffusion coefficient in cervical cancer of the uterus: comparison with the normal uterine cervix. *Eur Radiol.* 2005;15(1):71-8. DOI: 10.1007/s00330-004-2529-4.
24. McVeigh PZ, Syed AM, Milosevic M, Fyles A, and Haider MA. Diffusion-weighted MRI in cervical cancer. *Eur Radiol.* 2008;18(5):1058-64. DOI: 10.1007/s00330-007-0843-3.
25. Hou B, Xiang SF, Yao GD, et al. Diagnostic significance of diffusion-weighted MRI in patients with cervical cancer: a meta-analysis. *Tumour Biol.* 2014;35(12):11761-9. DOI: 10.1007/s13277-014-2290-5.
26. Liu Y, Ye Z, Sun H, and Bai R. Clinical Application of Diffusion-Weighted Magnetic Resonance Imaging in Uterine Cervical Cancer. *Int J Gynecol Cancer.* 2015;25(6):1073-8. DOI: 10.1097/IGC.0000000000000472.
27. Wang X, Song J, Zhou S, et al. A comparative study of methods for determining Intravoxel incoherent motion parameters in cervix cancer. *Cancer Imaging.* 2021;21(1):12. DOI: 10.1186/s40644-020-00377-0.
28. Ghardon SSL, Hemida R, Borg MA, Sallam HF, and Ahmed HM. Correlative study between apparent diffusion coefficient value and grading of cervical cancer. *Egyptian Journal of Radiology and Nuclear Medicine.* 2022;53(1):170.
29. Yang W, Qiang JW, Tian HP, Chen B, Wang AJ, and Zhao JG. Minimum apparent diffusion coefficient for predicting lymphovascular invasion in invasive cervical cancer. *J Magn Reson Imaging.* 2017;45(6):1771-79. DOI: 10.1002/jmri.25542.
30. Lura N, Wagner-Larsen KS, Ryste S, et al. Tumor ADC value predicts outcome and yields refined prognostication in uterine cervical cancer. *Cancer Imaging.* 2025;25(1):23.

This article is an open access article distributed under the terms and conditions of the Creative Commons Attribution (CC BY) license (<http://creativecommons.org/licenses/by/4.0/>).